Structural Engineering and Mechanics, *Vol. 54, No. 1 (2015) 121-133*
DOI: http://dx.doi.org/10.12989/sem.2015.54.1.121

Structural behavior of aluminum reticulated shell structures considering semi-rigid and skin effect

Hongbo Liu[1a], Zhihua Chen[*1], Shuai Xu[2] and Yidu Bu[2]

[1]State Key Laboratory Of Hydraulic Engineering Simulation And Safety, Tianjin University, Tianjin 300072, China
[2]School of Civil Engineering, Tianjin University, Tianjin 300072, China

(Received April 21, 2014, Revised November 9, 2014, Accepted December 16, 2014)

Abstract. The aluminum dome has been widely used in natatorium, oil storage tank, power plant, coal, as well as other industrial buildings and structures. However, few research has focused on the structural behavior and design method of this dome. At present, most designs of aluminum alloy domes have referred to theories and methods of steel spatial structures. However, aluminum domes and steel domes have many differences, such as elasticity moduli, roof structures, and joint rigidities, which make the design and analysis method of steel spatial structures not fully suitable for aluminum alloy dome structures. In this study, a stability analysis method, which can consider structural imperfection, member initial curvature, semi-rigid joint, and skin effect, was presented and used to study the stability behavior of aluminum dome structures. In addition, some meaningful conclusions were obtained, which could be used in future designs and analyses of aluminum domes.

Keywords: aluminum dome; structure type; stability; semi-rigid; skin effect; member initial curvature

1. Introduction

Aluminum alloy, steel, and concrete are the three main materials used in spatial structures. Concrete typically has a low strength-to-weight ratio; thus, the span of concrete structures is usually below 60 m. Steel is the preferred material for large-span structures because of the high strength-to-weight ratio, relatively mature design methodology, and construction technique. However, aluminum alloy has been the fastest growing structural material with the production increase and the cost reduction. According to Mazzolani (2012), Yang *et al*. (2013), Zhang *et al*. (2009), more than 6000 spatial structures worldwide have used aluminum alloy materials as the main structural member.

Using aluminum alloy as a structural material has many advantages, such as high strength-to-weight ratio, lightness, corrosion resistance, and ease of production. However, Young's modulus of aluminum is roughly one third of steel, which may cause the aluminum member to fail through buckling easily; and the thermal expansion coefficient of aluminum is roughly two times

*Corresponding author, Associate Professor, E-mail: zhchen@tju.edu.cn
[a]Associate Professor, E-mail: hbliu@tju.edu.cn

http://www.techno-press.org/?journal=sem&subpage=8 ISSN: 1225-4568 (Print), 1598-6217 (Online)

Table 1 Comparison of the main mechanical performance of aluminum and steel

	Density(kg/m^3)	Elasticity modulus (Mpa)	Expansion coefficient (/℃)	Poissons ratio
Aluminum alloy	2700	70000	24×10^{-6}	0.3
Steel	7850	206000	12×10^{-6}	0.26

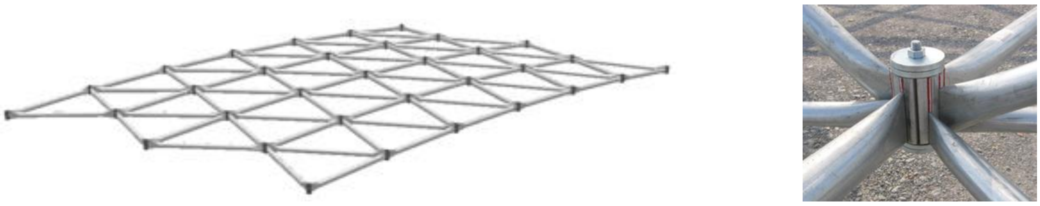

(a) single-layer

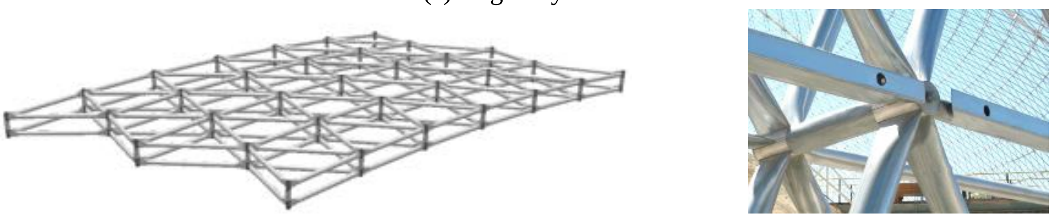

(b) double-layer-vierendeel

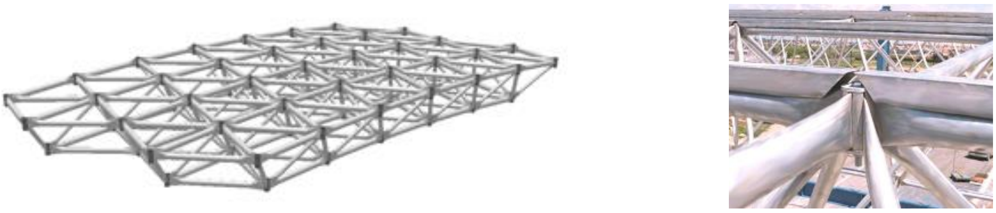

(c) double-layer-truss

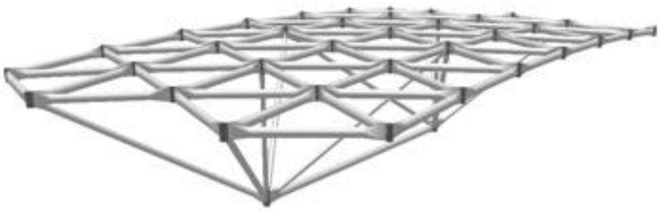

(d) ribbed

Fig. 1 Hub joint domes

of steel, which may cause the aluminum member to become sensitive to temperature change. The material mechanical performance of aluminum alloy and steel are listed in Table 1, which refers to the published papers of Mazzolani (2012), Yang *et al*. (2013), Zhang *et al*. (2009).

In recent years, aluminum alloy members have been used increasingly in structures. The current American Aluminum Design Manual (AA, 2005), Australian/New Zealand Standard Standards Australia (1997), and Eurocode EC9 “Design of Aluminium Structures” by the Technical Committee CEN-TC 250/SC9 for aluminum structures provide design rules for aluminum members. Jandaghi Shahi *et al*. (2012), Zhu *et al*. (2006, 2008) conducted many studies on axial compression performances. Zhu *et al*. (2006), Kim *et al*. (2010) also studied bending performance. Atzori *et al*. (1997), Fogle *et al*. (2012) studied anti-fatigue performance and anti-corrosion performance, respectively. May *et al*. (2005), Shi *et al*. (2012), Zhu *et al*. (2007) conducted studies on the bolted and welded joint performances of aluminum alloy members under axial compression and bending. However, few papers refer to the structural behavior of aluminum alloy dome structures (Hiyama 2000, Nanda 2005), which is a main structural type used in practice. In this study, a combined element that consisted of beam and spring elements was presented to simulate the initial curvature and joint semi-rigidity. The shell element was also used to study the effect of roof panel on the stability of aluminum alloy domes.

2. Structural forms of aluminum alloy structures

Aluminum alloy domes have two main types. One type is the hub joint dome, as shown in Fig. 1, and the other is the plate joint/gusset joint dome, as shown in Fig. 2.

Hub joint domes may be single-layer, double-layer-vierendeel, double-layer-truss, or ribbed, depending on the number of chord element layers. Single-layer geometries are used for moderate spans and architectural applications. Vierendeel geometries can be used for most circular and free-form domes. Vierendeel geometries are double-layer frames with parallel nodes in each layer that are connected with post members perpendicular to the surface of the dome. The second layer increases the bending strength and the buckling resistance without introducing unnecessary web elements. Double-layer truss geometries are used for large or concentrated loads, column supports, or extremely long spans. Ribbed geometries are also used in domes. They are easy to install because most of the assembly work may be done on the ground and lifted into place. Both the double-layer truss and the ribbed geometries may result in large chord densities.

This beam extrusion of the aluminum dome is typical. The protrusions on the top are the attachments for the dome panels and batten bar. The batten bar holds the dome panels in place and is attached using a 1/4” tri-lobe screw in the slot at the center of the beam. The flange stiffeners at the end of each flange are typical for thin-wall beam extrusions. The flange stiffeners increase the allowable compression and bending in a thin-wall shape by about 20%-25%. They also increase the weak-axis moment of inertia, section modulus, and gyration radius without increasing the beam width. They are not needed on thicker shapes.

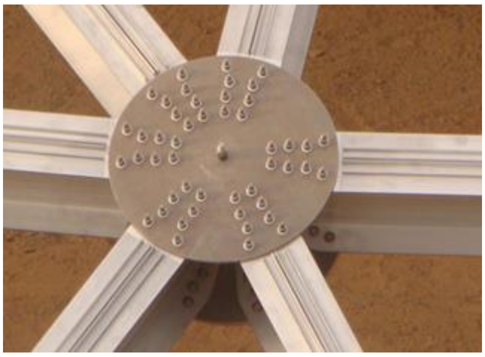

Fig. 2 Cover joint domes

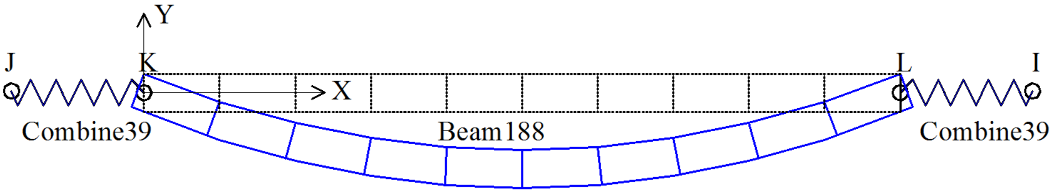

Fig. 3 Stimulating each member with 10 BEAM188 elements and two COMBINE39 elements

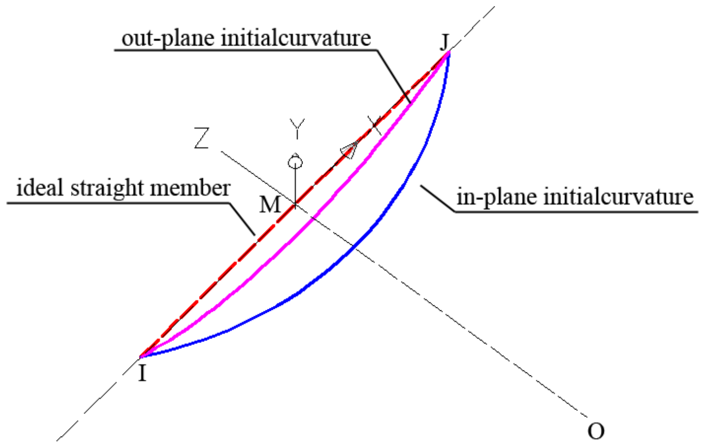

Fig. 4 Definition of the initial curvature of the aluminum member

The hubs are the connections where the beams are joined. The hub is a circular dish with a center hole punched in to be able to place the hub on the forming die to coin the angle needed for the dish. The center hole is tapped on the top hub to attach the hub cover. Four possible common aluminum materials can be used for the hubs: 6061-T6 extruded flat bar, 6063-T6 extruded flat bar, 6061-T6 hot-rolled plate, and 5052-H34 hot-rolled plate.

3. Finite element model for the aluminum domes

The current stability analysis and design method for aluminum domes assume that: 1) each member is straight; 2) the joint is rigid or hinged; 3) the effect of aluminum roof panels was ignored. However, the members have initial geometrical imperfections, which can obviously decrease the stability capacity. The presented joints are neither rigid nor hinged but semi-rigid. Furthermore, the aluminum roof panels above the structural member can prevent the local instability of the member and improve the stability capacity. To analyze the stability of aluminum domes accurately, an improved FE model using ANSYS software was presented in this study.

To consider the member initial curvature and joint semi-rigid, a combined multi-segment element with a beam element (BEAM188) and a spring element (COMBINE39) was presented in ANSYS software, which is shown in Fig. 3. The COMBIN39 element is 3D spring elements with a unidirectional freedom and nonlinear character, which were used to simulate the bending and torsional capacity of semi-rigid joints through integrating COMBIN39 real constants. BEAM188

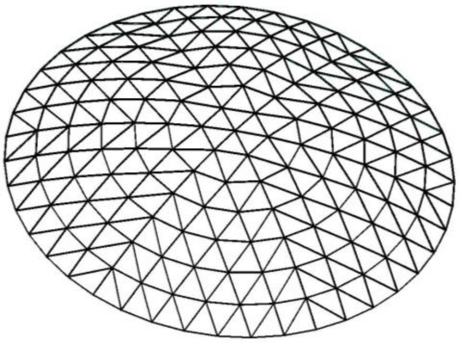

(a) Member without initial curvature

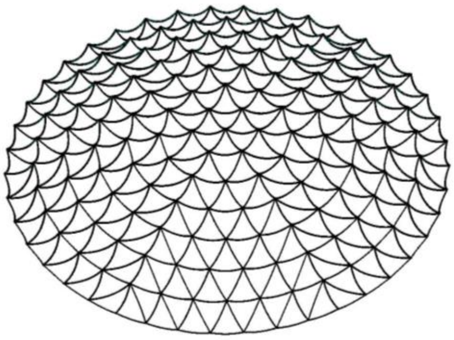

(b) Member with in-plane initial curvature

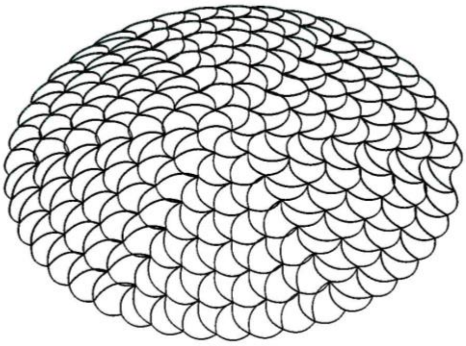

(c) Member with out-plane initial curvature

Fig. 5 FE model with member initial curvature

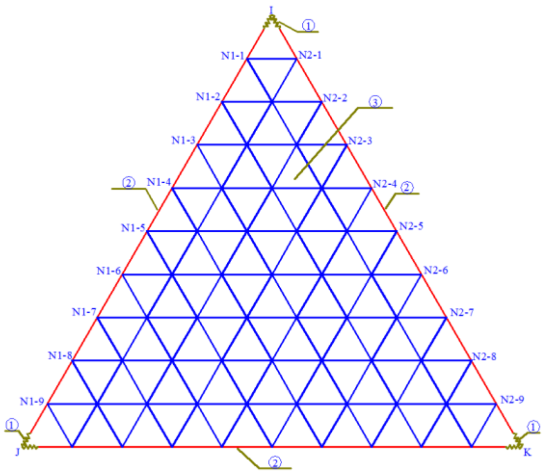

1:COMBINE39, 2:BEAM188, 3:SHELL181

Fig. 6 Schematic drawing for the FE model with upper roof aluminum panels

element is a 3D linear finite strain beam element based on Timoshenko beam theory and is suitable for analyzing slender to moderately stubby thick beam structures while considering the shear deformation effects, which were used to simulate the aluminum member. As shown in Fig. 4, each aluminum member was simulated with 10 Beam 188 elements to simulate the initial curvature. Two curvature types, out-web plane curvature and in-web plane curvature, were considered in this paper, as shown in Fig. 5. The curvature was assumed as $y=v_0x(x-L)$ and its maximum amplitude is $v_0=L/1000$.

SHELL181 element was used to simulate the aluminum panels that were above the H-sectional aluminum members, as shown in Fig. 6.

4. Structural behavior of aluminum domes

4.1 The studied model

To study the stability of an aluminum dome with a cover joint, a single-layer aluminum dome with span of 60 m was used, as shown in Fig. 7. The H-sectional members (H300×200×8×10) were adopted as the structural members. The members were connected with a cover joint, which was a semi-rigid joint. Grade T6160 aluminum was adopted.

4.2 Effect of initial imperfection and load distribution on stability behavior

Two models were designed to study the effect of structural initial imperfection on the stability of aluminum dome. One model had no structural initial imperfection and the other had structural imperfection. Based on consistent mode imperfection method, the initial imperfection model was determined using the first-order mode of the eigenvalue buckling with a maximum displacement value of L/300 (L is the span of dome). Meanwhile, two corresponding steel dome models with the same geometric size and the same member size were analyzed to compare the stability behaviors of the steel dome. The load-displacement curves and failure shape of the four models are shown in Figs. 8 and 9, and the following conclusions are obtained:

• The stability capacity of an aluminum dome with value of 5.25 kN/m^2 is 37.61% of the corresponding steel dome with a value of 13.96 kN/m^2 when no initial imperfection is present because of the decrease in the elasticity modulus by two-thirds; the stability bearing of an aluminum dome with value of 2.29 kN/m^2 is 25.33% of the corresponding steel dome with a value

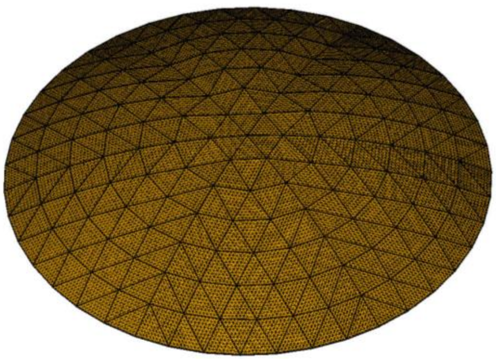

(a) the whole model

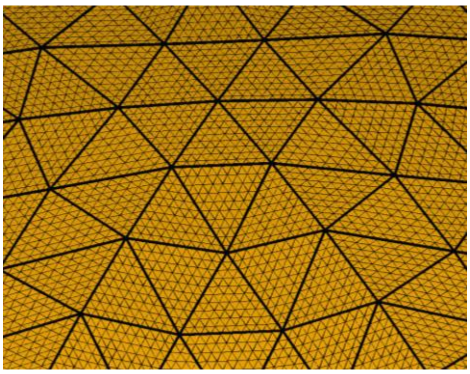

(b) the local model

Fig. 7 FE model with upper roof aluminum panels

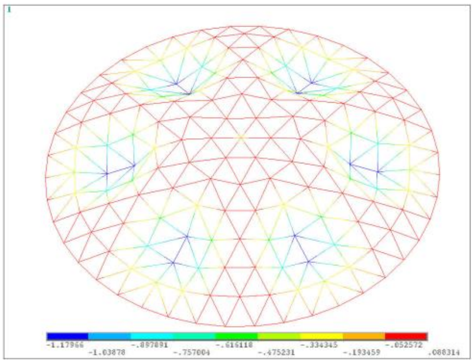

(a) steel, without initial imperfection

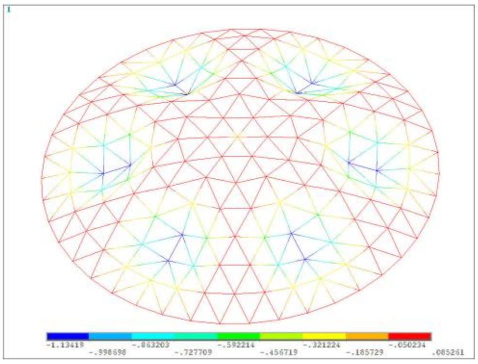

(b) aluminum, without initial imperfection

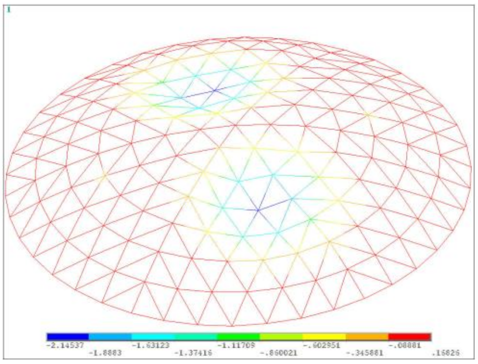

(c) steel, with initial imperfection

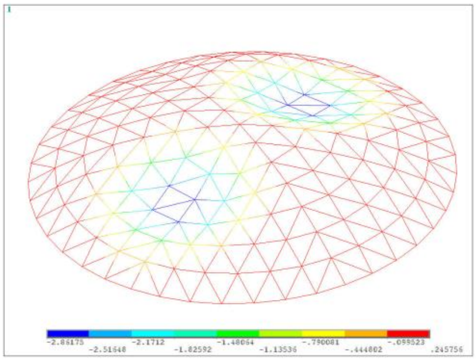

(d) aluminum, with initial imperfection

Fig. 8 Elastic failure modes of an aluminum and steel dome

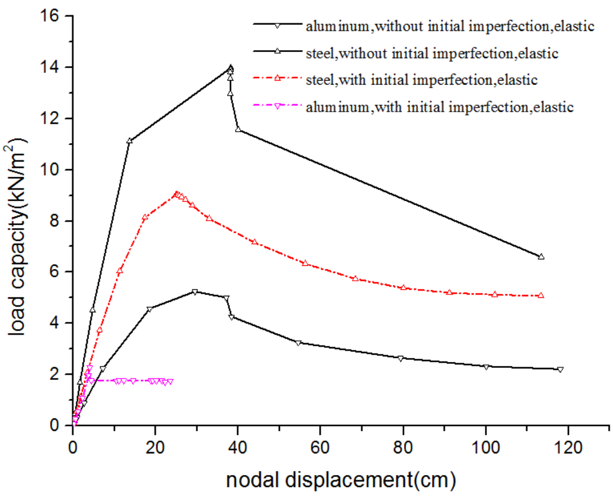

Fig. 9 Load-displacement curve of an aluminum dome that considers initial imperfection

of 9.04 kN/m^2 when initial imperfection is present. Therefore, the stability of an aluminum dome is weaker than that of a steel dome.

• The stability bearing capacity of an aluminum dome has fallen by 56.38% when the initial

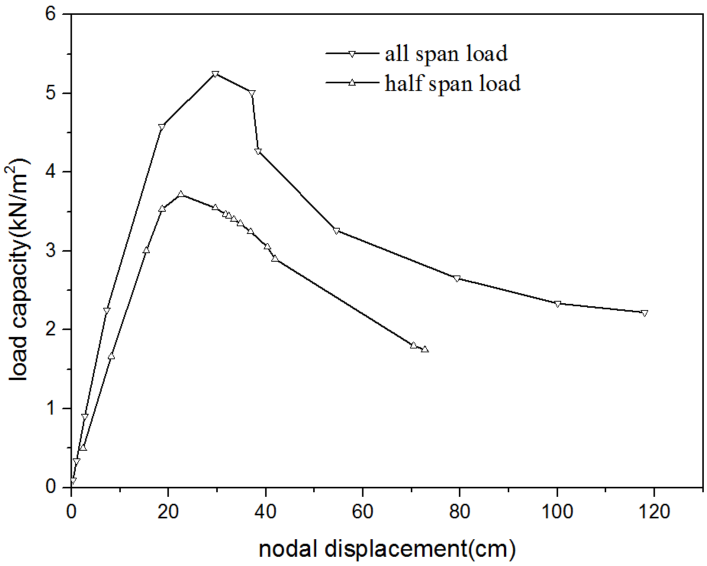

Fig. 10 Load-displacement curve of an aluminum dome under an all and half-load distribution

imperfection is considered, which is 1.60 times than that of the corresponding steel dome with a value of 35.24%. Therefore, the aluminum dome is more sensitive to structural initial imperfections than the steel dome.

Two models were designed to study the effect of load distribution on the stability of an aluminum dome. One model is under all span loading, and the other is under half-span loading. The load-displacement curves and failure shape of the two models are shown in Fig. 10. The stability capacity under half-span loading is approximately 29.33% lower than that under all-span loading.

4.3 Effect of material elasto-plastic on stability behavior

To study the elasto-plastic behavior of aluminum and steel on the stability, the elasto-plastic stability of aluminum domes and steel domes were analyzed using an ideal elasto-plastic model, which is shown in Fig. 11. The initial imperfection was also considered in this section. The values of the elasticity moduli and yielding strengths for steel and aluminum are listed in Table 1. The results are shown in Figs. 12 and 13. The stability of an aluminum dome has little change with the values of 2.13 kN/m^2 and 2.29 kN/m^2 when considering material elasto-plastic property or not. However, the stability of a steel dome has fallen 57.41% from 9.04 kN/m^2 to 3.85 kN/m^2. Thus, the failure mode of an aluminum dome is buckling and not yielding.

Based on the results of Section 4.2 and Section 4.3, a remarkable difference between steel domes and aluminum domes, and two suggestions were given as follows in the stability design of the aluminum dome:

• The elasto-plastic stability analysis of an aluminum dome may be omitted in the stability design process because the dome will always buckle and not yield;

•The construction precision of an aluminum dome is stricter than that of a steel dome because an aluminum dome is sensitive to initial imperfection.

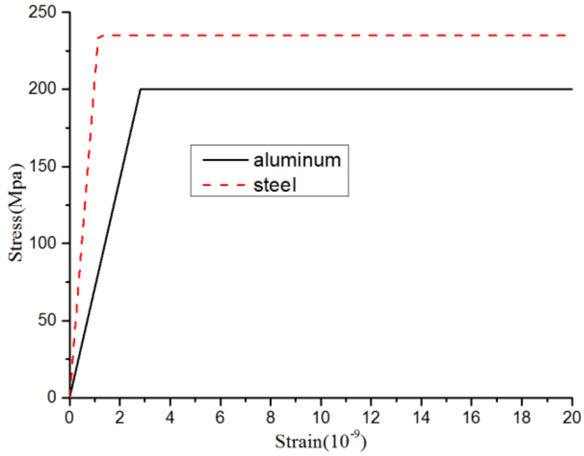

Fig. 11 The ideal elasto-plastic model of aluminum and steel used in this study

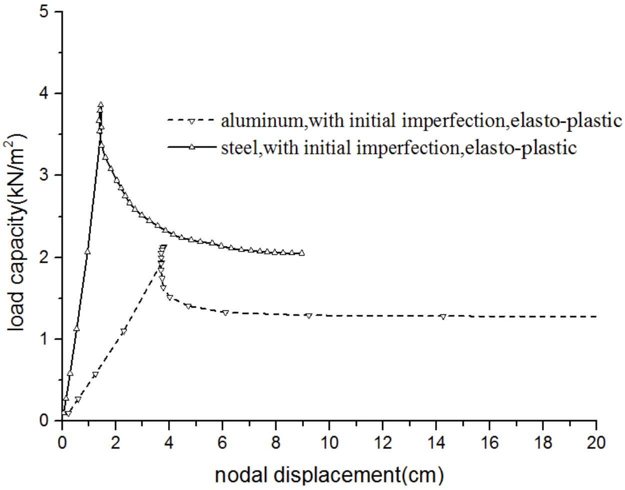

Fig. 12 Load-displacement curve of an aluminum dome considering elasto-plastic

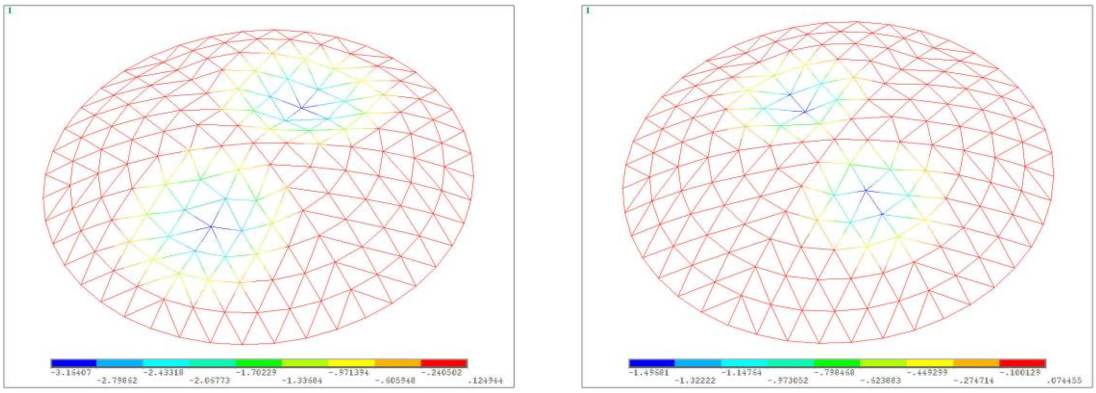

(a) steel, with initial imperfection (b) aluminum, with initial imperfection

Fig. 13 Elasto-plastic failure modes of aluminum dome

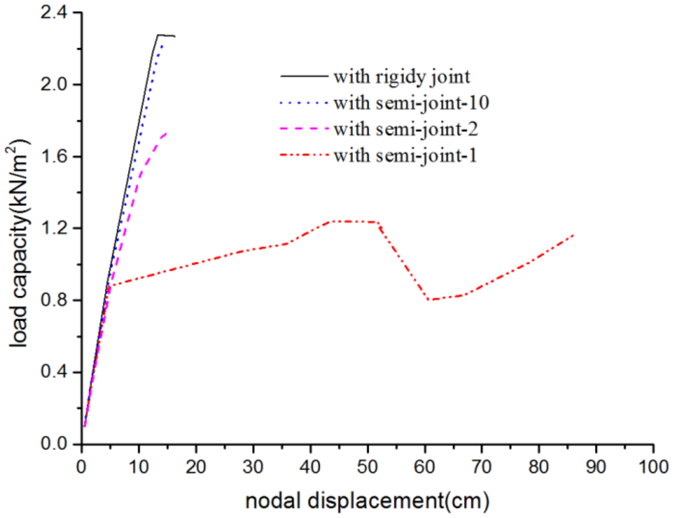

Fig. 14 Load-displacement curve of aluminum dome considering semi-rigidity

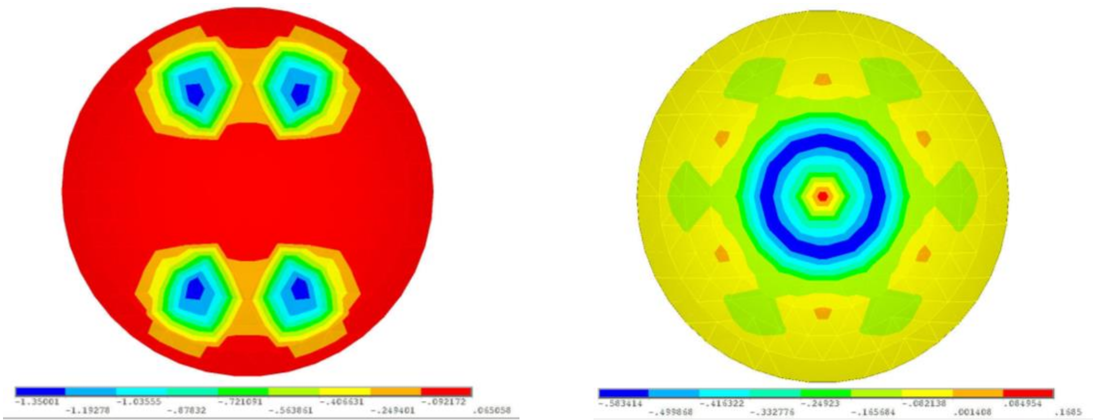

(a) rigid joint (b) semi-rigid joint

Fig. 15 Failure modes of aluminum dome considering joint rigidity

4.4 Effect of joint rigidity on stability behavior

For most single-layer lattice aluminum domes, the cover joint shown in Fig. 2 was adopted. On the basis of the experimental data and numerical analysis, we conclude that the cover joint is neither hinged nor fixed but a semi-rigid joint. One circle cover plate joint was statically tested in the structural laboratory of Tianjin University (Bu 2013). Based on the test data, the in-plane rotational stiffness is 2312 kN·m/rad and the out-plane rotational stiffness is 273 kN·m/rad. Four models with different joint rotational stiffnesses were designed to study the effect of joint rotational stiffness. Their rotational stiffnesses are a one-time test value, two-time test value, ten-time test value, and completely rigid, respectively. Using the method presented in Section 3, the stability of aluminum domes that consider the semi-rigidity behavior was analyzed, and the result is shown Figs. 14 and 15. The stability capacities of the four studied models were 1.24 kN/m^2,

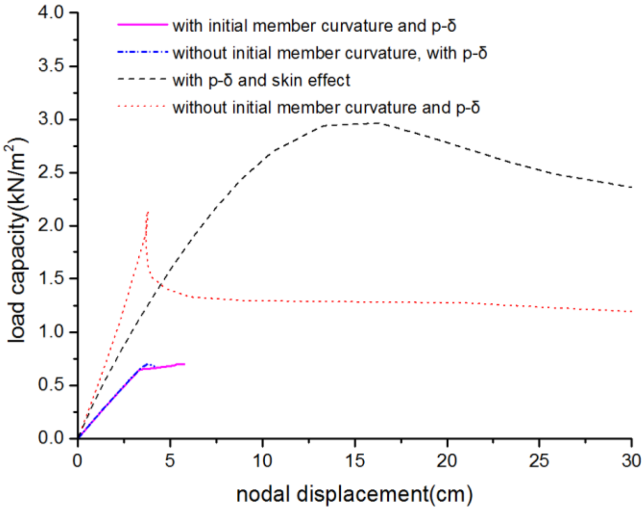

Fig. 16 Load-displacement curve of aluminum dome considering *p-δ* effect, member initial curvature, and skin effect

1.75 kN/m^2, 2.25 kN/m^2 and 2.28 kN/m^2. The stability capacity increases with the joint rotational stiffness. The stability capacity of aluminum dome with a one-time test stiffness is 54.39% of the aluminum dome with a completely rigid joint. Therefore, the semi-rigidity property of the circle cover plate joint must be considered for future analysis.

4.5 Effect of member initial curvature and skin on stability behavior

For spatial structures, the stability analysis has two aspects, which are structural stability and member stability. In most presented stability analyses, the member stability is usually ignored, and the result cannot show the actual failure state. In this section, the member stability and initial member curvature were considered using the method presented in Section 3. The H-section member cannot buckle around the weak axis because the aluminum plate above the H-section member is firmly connected with the H-section member. Therefore, the initial curvature around the weak axis was ignored. Furthermore, the effect of the aluminum plate above the H-section member on stability was considered using the method presented in Section 3. The analysis results are shown in Fig. 16 and the following conclusions were obtained:

•Considering the *p-δ* effect of the member, the stability-bearing capacity fell by 43.55% from 1.24 kN/m^2 to 0.7 kN/m^2. Therefore, the member *p-δ* has a remarkable effect on stability;

• The member initial curvature has little effect on the stability-bearing capacity;

• Considering the skin effect, the stability-bearing capacity increased by 322.86% from 0.70 kN/m^2 to 2.96 kN/m^2. Therefore, the effects of the upper aluminum plate are suggested for future analysis.

5. Conclusions

• The structural forms of the existing aluminum alloy dome were summarized.

• A stability analysis method, which can consider structural imperfection, member initial curvature, semi-rigid joint, and skin effect, was presented and used to study the stability behavior of aluminum dome structures.

• The stability bearing of the aluminum dome was about one-third of the corresponding steel dome because the elasticity modulus dropped by two-thirds; the stability-bearing capacity fell by 56.38% when the initial imperfection was considered. Therefore, the aluminum dome is sensitive to structural initial imperfection.

• The stability of aluminum dome changed little whether the material elasto-plastic property was considered or not. Therefore, the aluminum dome usually buckles and not yields under a uniform load.

• The stability of the aluminum dome fell by 54.39% when the semi-rigidity behavior was considered. Therefore, the joint semi-rigidity behavior has a remarkable effect on stability behavior.

• Considering the p-δ effect of the member, the stability-bearing capacity fell by 43.55%. Considering the skin effect, the stability-bearing capacity increased by 322.86%. Therefore, the p-δ of member and skin effect of the upper aluminum plate has a remarkable effect on stability behavior.

Acknowledgments

This work was supported by the higher school special funds for authors of the National Excellent Doctoral Dissertation (No. 201453) and the China Postdoctoral Science Foundation Funded Project (No. 2013T60253).

References

Atzori, B., Lazzarin, P. and Quaresimin, M. (1997), “A re-analysis on fatigue data of aluminium alloy bolted joints”, *Int. J. Fatig.*, **19**(7), 579-588.

Bu, Y.D. (2013), “Structural mechanical property analysis of coal storage aluminum alloy dome in Caofeidian”, Master Degree Thesis of Tianjin University, China, Tianjin City.

Fogle, E.J., Lattimer, B.Y., Feih, S., Kandare, E., Mouritz, A.P. and Case, S.W. (2012), “Compression load failure of aluminum plates due to fire”, *Eng. Struct.*, **34**, 155-162.

Hiyama, Y., Ishikawa, K. and Kato, S. (2000), “Experiments and analysis of the post-buckling behaviors of aluminum alloy double layer space grids applying ball joints”, *Struct. Eng. Mech.*, **9**(3), 289-304.

Jandaghi Shahi, V. and Marzbanrad, J. (2012), “Analytical and experimental studies on quasi-static axial crush behavior of thin-walled tailor-made aluminum tubes”, *Thin Wall. Struct.*, **60**, 24-37.

Kim, Y. and Peköz, T. (2010), “Ultimate flexural strength of aluminum sections”, *Thin Wall. Struct.*, **48**(10), 857-865.

May, J.E. and Menzemer, C.C. (2005), “Strength of bolted aluminum alloy tension members”, *J. Struct. Eng.*, **131**(7), 1125-1134.

Mazzolani, F.M. (2012), “3D aluminium structures”, *Thin Wall. Struct.*, **61**(SI), 258-266.

Nanda, B.K. and Behera, A.K. (2005), “Study on structural damping of aluminium using multi-layered and jointed construction”, *Struct. Eng. Mech.*, **20**(6), 631-653.

Shi, G., Luo, C., Wang, Y., Shi, Y. and Li, G. (2012), “Experimental study on mechanical performance of novel cast aluminum joints in aluminum reticulated shell structures”, *J. Build. Struct.*, **33**(3), 70-79.

Yang, L., Wei, S. and Zhang, Q. (2013), “Aluminum reticulated spatial structures: state of the art and key issues", *J. Build. Struct*., **34**(2), 1-20.

Zhang, Q., Ji, J., Yang, L. and Wu, M. (2009), "Some important concepts and research bases of Code for Design of Aluminum Structures", *J. Build. Struct*., **30**(5), 1-12.

Zhu, J.H. and Young, B. (2009), "Design of aluminum alloy flexural members using direct strength method", *J. Struct. Eng*., **135**(5), 558-566.

Zhu, J.H. and Young, B. (2008), "Numerical investigation and design of aluminum alloy circular hollow section columns", *Thin Wall. Struct*., **46**(12), 1437-1449.

Zhu, J.H. and Young, B. (2006), "Tests and design of aluminum alloy compression members", *J. Struct. Eng*., **132**(7), 1096-1107.

Zhu, J.H. and Young, B. (2006), "Aluminum alloy circular hollow section beam-columns", *Thin Wall. Struct*., **44**(2), 131-140.

Zhu, J.H. and Young, B. (2006), "Experimental investigation of aluminum alloy thin-walled tubular members in combined compression and bending", *J. Struct. Eng*., **132**(12), 1955-1966.

Zhu, J.H. and Young, B. (2007), "Effects of transverse welds on aluminum alloy columns", *Thin wall. Struct*., **45**(3), 321-329.

http://www.geometrica.com/en/domes

CC